Brief Articles

Structures of the Ligand-Binding Core of iGluR2 in Complex with the Agonists (*R*)- and (*S*)-2-Amino-3-(4-hydroxy-1,2,5-thiadiazol-3-yl)propionic Acid Explain Their Unusual Equipotency[⊥]

Mads Beich-Frandsen,[§,†] Darryl S. Pickering,[#] Osman Mirza,[§] Tommy N. Johansen,[‡] Jeremy Greenwood,[§] Bente Vestergaard,[§] Arne Schousboe,[#] Michael Gajhede,[§] Tommy Liljefors,[§] and Jette S. Kastrup*[,§]

Department of Medicinal Chemistry (Biostructural Research), Department of Medicinal Chemistry (Neuromedicinal Chemistry), and Department of Pharmacology and Pharmacotherapy, Faculty of Pharmaceutical Sciences, University of Copenhagen, Universitetsparken 2, DK-2100 Copenhagen, Denmark

Received September 11, 2007

AMPA-type ionotropic glutamate receptors generally display high stereoselectivity in agonist binding. However, the stereoisomers of 2-amino-3-(4-hydroxy-1,2,5-thiadiazol-3-yl)propionic acid (TDPA) have similar enantiopharmacology. To understand this observation, we have determined the X-ray structures of (*R*)-TDPA and (*S*)-TDPA in complex with the ligand-binding core of iGluR2 and investigated the binding pharmacology at AMPA and kainate receptors. Both enantiomers induce full domain closure in iGluR2 but adopt different conformations when binding to the receptor, which may explain the similar enantiopharmacology.

Introduction

(*S*)-glutamate is the main excitatory amino acid in the central nervous system and mediates fast synaptic transmission by its binding to three different classes of ionotropic glutamate receptors (iGluRs[a]), designated 2-amino-3-(3-hydroxy-5-methyl-4-isoxazolyl)propionic acid (AMPA), kainic acid (KA), and *N*-methyl-D-aspartic acid (NMDA) receptors.[1] The glutamatergic system is involved in various aspects of normal brain function but is also implicated in a variety of brain disorders. Hence, it is a potential target for pharmacotherapy.[1,2]

The iGluRs are ligand-gated ion channels composed of four subunits forming a pair of dimers.[3] Each subunit comprises an extracellular N-terminal domain, a ligand-binding core made of segments S1 and S2, three transmembrane spanning regions (M1−M3) and a re-entrant loop (P) between M1 and M2 as well as a cytoplasmic region. A soluble form of the ligand-binding core of iGluR2 (iGluR2-S1S2J) has been prepared, belonging to the AMPA class of iGluRs.[4] A number of structures of iGluR2-S1S2J in complex with various agonists[4–7] and antagonists[4,8,9] have been determined within recent years. The ligands bind in a cleft between two domains, D1 and D2, composed primarily of residues from segments S1 and S2, respectively. Domain movement occurs upon ligand binding, which results in closure of the binding cleft. The extent of domain closure is correlated to the activation and desensitization of the receptor.[6,7]

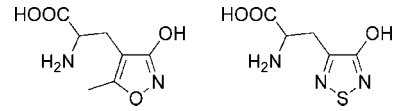

Figure 1. Structures of AMPA (left) and TDPA (right).

Generally, a high degree of agonist stereoselectivity is observed at the AMPA class of receptors. Intrigued by the fact that the stereoisomers of 2-amino-3-(4-hydroxy-1,2,5-thiadiazol-3-yl)propionic acid (TDPA; see Figure 1) are approximately equipotent,[10] we investigated the binding of (*R*)-TDPA and (*S*)-TDPA to the ligand-binding core of iGluR2 at the molecular level. Here, the two complex structures are presented, as determined by X-ray crystallography. In addition, the binding pharmacology of both enantiomers at iGluR2-S1S2J and at the full-length receptors iGluR1–6 has been determined.

Results

Structure of the iGluR2-S1S2J/(*R*)-TDPA Complex. The structure was determined to 1.95 Å resolution and contains four molecules (denoted MolA-D) of iGluR2-S1S2J in complex with (*R*)-TDPA in the asymmetric unit of the crystal. (*R*)-TDPA introduces full domain closure in all four iGluR2-S1S2J molecules (MolA, 20°; MolB, 19°; MolC, 20°; MolD, 19°; calculated relative to the apo structure of iGluR2-S1S2J, MolA, PDB code 1FTO[4]). Also, (*R*)-TDPA binds in a similar way to the ligand-binding cleft in all molecules. The interactions of the α-amino acid part of the ligand with the receptor are very similar to those of other agonists[4,5,11] (see Figure 2a, Table 1, and Supporting Information (SI) Table 3. The heterocyclic ring

[⊥] PDB codes for iGluR2-S1S2J complexes (*R*)-TDPA and (*S*)-TDPA are 3BFU and 3BFT, respectively.

* To whom correspondence should be addressed. Phone: +45 35 33 64 86. Fax: +45 35 33 60 40. E-mail: jsk@farma.ku.dk.

[§] Department of Medicinal Chemistry (Biostructural Research).

[†] Present address: Max F. Perutz Laboratories, University Departments at the Vienna Biocenter, Department for Biomolecular Structural Chemistry, Faculty of Chemistry, University of Vienna, Campus Vienna Biocenter 5, A-1030 Vienna, Austria.

[#] Department of Pharmacology and Pharmacotherapy.

[‡] Department of Medicinal Chemistry (Neuromedicinal Chemistry).

[a] Abbreviations: AMPA, 2-amino-3-(3-hydroxy-5-methyl-4-isoxazolyl)-propionic acid; iGluR, ionotropic glutamate receptor; iGluR2-S1S2J: ligand-binding core construct of iGluR2; TDPA, 2-amino-3-(4-hydroxy-1,2,5-thiadiazol-3-yl)propionic acid.

10.1021/jm701126w CCC: $40.75
Published on Web 02/13/2008

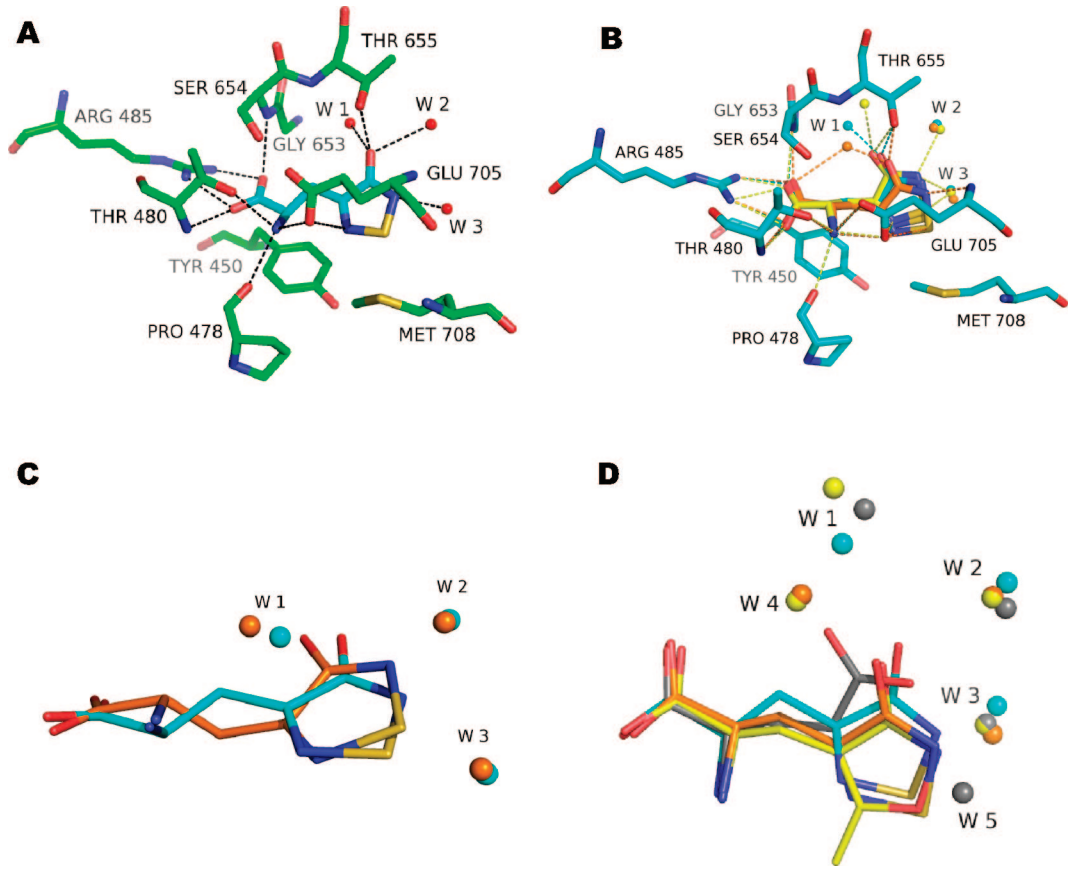

Figure 2. Ligand-binding site of iGluR2-S1S2J. (A) (*R*)-TDPA complex (MolA). Heteroatoms are in standard colors (nitrogen is blue, oxygen is red, and sulfur is yellow). (*R*)-TDPA is displayed in cyan and protein residues in green. Water molecules are shown as red spheres, and dashed lines indicate potential hydrogen bonds/ionic interactions listed in Table 1. (B) The (*S*)-TDPA complex. The three molecules of the asymmetric unit of the crystal have been superimposed. The ligand, water molecules, and potential hydrogen bonds/ionic interactions are colored cyan in MolA, orange in MolB, and yellow in MolC. Protein residues are shown for MolA only. The position of (*S*)-TDPA in MolB corresponds to that of (*S*)-AMPA in the iGluR2-S1S2J/AMPA complex (PDB code 1FTM) and in MolC approximately to that of (*S*)-glutamate in the iGluR2-S1S2J:glutamate complex (PDB code 1FTJ). In MolA, (*S*)-TDPA is located between the two extremes. (C) Superposition of (*R*)-TDPA (MolA, in cyan) and (*S*)-TDPA (MolA, in orange) complexes. For clarity, only the ligands and water molecules are shown. (D) Superposition of the (*R*)-TDPA (MolA, in cyan), (*S*)-TDPA (MolB, in orange), (*S*)-AMPA (PDB code 1FTM, MolA; in yellow), and (*S*)-glutamate (PDB code 1FTJ, MolA; in gray) complexes. For clarity, only the ligands and water molecules are shown.

of (*R*)-TDPA is positioned in a similar way to that of (*S*)-AMPA in the iGluR2-S1S2J complex.[4] However, the water molecule (W4), which is specific for agonists binding in the AMPA mode and which mediates contacts between ligand and protein, is not present in the (*R*)-TDPA complex. Instead, a water molecule (denoted W1) has been located between the two water molecules (W1 and W4) of the AMPA complex. In the present structure, W1 makes a hydrogen bond to the 3-hydroxy group of the isoxazole and is further connected to the amino acid residues Leu650 (N 2.8 Å) and Leu703 (O 2.6 Å). Similar contacts are formed between the γ-carboxylate of (*S*)-glutamate and W1 in the iGluR2-S1S2J complex.[4]

Structure of the iGluR2-S1S2J/(*S*)-TDPA Complex. The structure was determined to 2.25 Å resolution and contains three molecules (named MolA−C) in the asymmetric unit. Zn^{2+} ions are present in the structure, leading only to minor variations in loop conformations compared with the iGluR2-S1S2J/(*R*)-TDPA complex. This accords with previously reported observations.[11,12] As with (*R*)-TDPA, (*S*)-TDPA induces full domain closure of the ligand-binding core (MolA, 20°; MolB, 20°; MolC, 19°). Whereas the α-amino acid part of (*S*)-TDPA binds as observed for other agonists, the heterocyclic ring is located at slightly different positions in all three molecules, with the extremes corresponding almost to the AMPA and glutamate (γ-carboxylate) binding modes (Figure 2B). Accordingly, the water structure within the ligand-binding site is affected by this. In MolA, one water molecule (denoted W1) is located between W1 and W4 of the iGluR2-S1S2J/(*S*)-AMPA complex. In MolB, the position of this water molecule corresponds to that of W4 in the iGluR2-S1S2J/(*S*)-AMPA complex, whereas in MolC it is located similarly to W1 in the iGluR2-S1S2J/(*S*)-AMPA complex.

Comparison of (*R*)-TDPA and (*S*)-TDPA Complexes. The α-amino acid portions of (*R*)-TDPA and (*S*)-TDPA are located at the same positions in both structures, and this is also reflected in low *B* values (5–15 Å^2 in the (*R*)-TDPA complex and 20–31 Å^2 in the (*S*)-TDPA complex) of the α-amino acid portion in all molecules compared to the average *B* values (SI Figure 4). Higher *B* values (up to 25 Å^2 in the (*R*)-TDPA complex and up to 51 Å^2 in the (*S*)-TDPA complex) are seen in the distal regions of both ligands. The position of the distal part of (*R*)-TDPA resembles most closely that of (*S*)-TDPA in MolA (Figure 2C). In both structures, three structural water molecules (W1, W2, and W3) are located in the vicinity of the ligands. W1 is engaged in hydrogen-bonding networks from (*R*)-TDPA and (*S*)-TDPA to the protein, even though W1 is located at different positions in the three molecules of the (*S*)-TDPA complex. Mobility of W1 is also reflected in generally higher *B* values for W1 than W2 and W3 (SI Figure 4). Water molecules W2 and W3 are located at similar positions in the two TDPA structures, as well

Table 1. Interactions of (*R*)-TDPA and (*S*)-TDPA with the Ligand-Binding Core of iGluR2[a]

	(*R*)-TDPA	(*S*)-TDPA	(*S*)-AMPA	(*S*)-Glu
Carboxylate Oxygen 1				
Thr480 N	2.8	2.9	3.0	3.0
Arg485 Nη1	2.8	2.9	2.8	2.8
Carboxylate Oxygen 2				
Arg485 Nη2	2.8	2.6	3.0	2.9
Ser654 N	2.9	2.9	3.0	2.9
W4			2.9	
Ammonium Group				
Pro478 O	2.8	3.0	2.7	2.7
Thr480 Oγ1	2.9	3.0	3.0	3.0
Glu705 Oϵ1	2.8	2.7	2.7	2.7
Glu705 Oϵ2		3.1		
Distal Hydroxy Oxygen				
Thr655 Oγ1	2.5	2.6	2.7	2.7[c]
W1	2.8	2.4		3.1[b]
W2	3.0		3.0	3.0[c]
W4			2.5	
W5				2.8[c]
Heterocyclic Ring Nitrogen				
Glu705 N			3.1	
W3	3.0		3.0	

[a] Potential hydrogen bonds/ionic interactions (in Å) to ligands within 3.2 Å are tabulated. Interactions of (*S*)-AMPA and (*S*)-glutamate have been included for comparison. Molecule A was used in all cases. [b] Contacts to γ-carboxylate oxygen 1. [c] Contacts to γ-carboxylate oxygen 2.

as in the structures of iGluR2-S1S2J in complex with (*S*)-AMPA and (*S*)-glutamate, respectively (Figure 2D). In the (*S*)-TDPA complex, water-mediated hydrogen bonds from W2 and W3 only seem to play a minor role in anchoring the ligand (Table 2 and SI Table 3).

Pharmacology of (*R*)-TDPA and (*S*)-TDPA. No statistically significant difference between the affinities of (*R*)-TDPA and (*S*)-TDPA at iGluR2(*R*)$_o$ versus iGluR2-S1S2J was observed (Table 2). Among AMPA receptors, (*R*)-TDPA is slightly selective toward iGluR1/iGluR2 ($P < 0.001$, one-way ANOVA, Holm−Sidak post-test), while (*S*)-TDPA is nonselective. Only weak binding affinity is found at the kainate receptors iGluR5 and iGluR6. A comparison of the present structures with those of (*S*)-glutamate in complex with iGluR5-S1S2 (PDB code 1YCJ[13]) and iGluR6-S1S2 (PDB code 1S50[14]), respectively, suggests that the amino acid difference at position 708 in iGluR2 (Met versus Ser/Thr in iGluR5/iGluR6) is the major contributor to the large selectivity toward AMPA receptors (SI Table 4). In kainate receptors, binding of TDPA to the ligand-binding site will probably disrupt the water-mediated network originating from Ser/Thr.

Discussion

In general, a high degree of receptor stereoselectivity is observed for AMPA receptors. At native AMPA receptors, AMPA displays a more than 1000-fold stereoselectivity.[15] By contrast, (*R*)-TDPA and (*S*)-TDPA show similar affinities at native[10] and at cloned AMPA receptors (Table 2). Although the enantiomers of TDPA adopt different bioactive conformations when binding to iGluR2 (Figure 2C and SI Table 5), the binding modes are in good agreement with the calculated binding modes reported earlier,[15] with (*S*)-TDPA adopting a conformation similar to that displayed by (*S*)-AMPA[4] (SI Table 5). No X-ray structure of (*R*)-AMPA in complex with iGluR2 has been reported. However, in order for (*R*)-AMPA to be able to bind to iGluR2, while preserving the ligand–receptor interactions for the α-amino acid moiety seen in all studied iGluR2 agonist structures, it is reasonable to assume that the bioactive conformation of (*R*)-AMPA is similar to that of (*R*)-TDPA. Since AMPA has a methyl substituent at the 5-position, a conformation of (*R*)-AMPA similar to that of (*R*)-TDPA would most likely give strong steric repulsion and thus a large conformational energy penalty for binding. Since TDPA does not have a substituent in the corresponding position, the difference in the conformational energy penalties for the enantiomers should be much smaller than for AMPA, which would rationalize the different enantiopharmacologies of AMPA and TDPA.

To investigate this hypothesis, we have carried out calculations of the difference in conformational energy penalties for the enantiomers of TDPA compared with those of AMPA, assuming that the bioactive conformation of (*R*)-AMPA mimics that of (*R*)-TDPA (see SI). Relative conformational energy penalties of the (*R*)- and (*S*)-enantiomers of AMPA and TDPA were then calculated by subtracting the energies for the partially relaxed structures, excluding the solvation contributions. The relaxed structures of the TDPA and AMPA enantiomers and the calculated relative conformational energy penalties are shown in Figure 3. The large conformational energy penalty for the bioactive conformation of (*R*)-AMPA compared to that of (*S*)-AMPA is due to repulsive steric interactions between the ammonium group and the methyl group in (*R*)-AMPA. Note that the methyl group of AMPA was not subjected to any constraints in the calculations (see SI). These repulsive interactions cannot be significantly relieved if (*R*)-AMPA is to display interactions with the iGluR2 receptor similar to those displayed by other iGluR2 agonists, which is consistent with the low affinity of (*R*)-AMPA. By contrast, (*R*)-TDPA and (*S*)-TDPA show similar calculated conformational energy penalties in agreement with the small difference in affinities for the enantiomers (Figure 3). Thus, the absence of significant enantioselectivity of TDPA may be rationalized by the small difference in conformational energies of the bioactive conformations of the enantiomers.

Experimental Section

Materials. The synthesis and resolution of (*R*)-TDPA and (*S*)-TDPA are as described.[10] Stereochemical purity of both enantiomers was higher than 99.8% ee. Chemicals were purchased from Sigma-Aldrich (Vallensbæk Strand, Denmark) unless otherwise specified.

Protein Expression and Purification. The iGluR2-S1S2J construct described by Armstrong and Gouaux[4] was expressed, refolded, and purified essentially as previously reported.[16] Full-length iGluR1$_o$, iGluR2(*R*)$_o$, iGluR3$_o$, iGluR4$_o$, iGluR5(Q), and iGluR6(V,C,R) were expressed in Sf9 insect cells. Cells were maintained in BaculoGold Max-XP serum-free medium (BD

Table 2. Binding Affinities of (*R*)-TDPA and (*S*)-TDPA at iGluR2-S1S2J and Full-Length Receptors

	K_i (nM)[a]						
	iGluR2-S1S2J	iGluR1$_o$	iGluR2$_o$(R)	iGluR3$_o$	iGluR4$_o$	iGluR5(Q)	iGluR6(V,C,R)
(*R*)-TDPA	531 ± 98	150 ± 26	234 ± 12	1070 ± 120	1055 ± 165	>10000	>1000000
(*S*)-TDPA	323 ± 84	185 ± 15	273 ± 37	160 ± 18	182 ± 10	18500 ± 1500	>100000

[a] Mean ± SEM from at least three individual experiments, conducted in triplicate. Hill coefficients were close to unity in all cases.

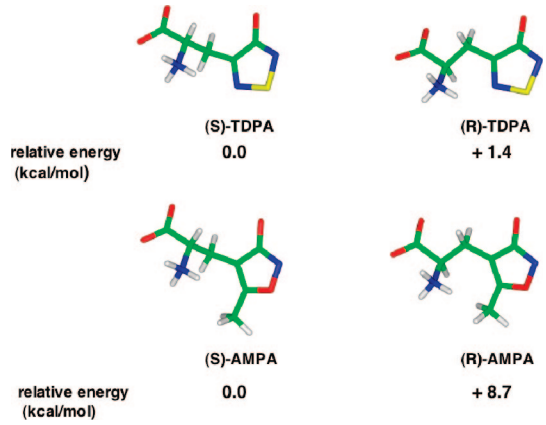

Figure 3. Partially relaxed structures and calculated relative conformational energy penalties for the enantiomers of TDPA and AMPA.

Biosciences, Pharmingen, San Diego, CA) according to standard protocols in "Guide to Baculovirus Expression Vector Systems and Insect Cell CultureTechniques" (Life Technologies, Paisley, U.K.) and "Baculovirus Expression Vector System: Procedures and Methods Manual", 2nd edition (Pharmingen).

Receptor Binding. The affinities of (*R*)-TDPA and (*S*)-TDPA at the soluble iGluR2-S1S2J construct and at full-length iGluR1$_o$, iGluR2(R)$_o$, iGluR3$_o$, iGluR4$_o$, iGluR5(Q), and iGluR6(V,C,R) receptors were determined by radioligand-binding assay, as previously described.[17,18]

Cocrystallization of iGluR2-S1S2J with (*R*)-TDPA and (*S*)-TDPA. The iGluR2-S1S2J protein was dialyzed extensively in crystallization buffer (10 mM Hepes, pH 7.0, 20 mM NaCl, 1 mM EDTA) and concentrated to 7.5 mg/mL. The iGluR2-S1S2J protein was mixed with (*R*)-TDPA or (*S*)-TDPA at a ratio of 1:30. Crystals were obtained at 6 °C by the hanging drop vapor diffusion method. For (*R*)-TDPA, a reservoir solution containing 18% polyethylene glycol monomethyl ether 2000 (PEG-MME 2K), 0.1 M cacodylate, pH 6.5, and 0.2 M ammonium sulfate was used, and for (*S*)-TDPA 22% PEG-MME 2K, 0.1 M cacodylate, pH 6.5, and 0.2 M zinc acetate. Crystals were transferred through a cryoprotectant solution consisting of 20% glycerol in reservoir solution prior to flash-cooling at 110 K.

X-ray Data Collection. The X-ray diffraction data of the (*R*)-TDPA complex were collected at cryogenic temperature and at a wavelength of 0.8122 Å at beamline BL1 (BESSY, Berlin, Germany). For the (*S*)-TDPA complex, data were collected at beamline X11 (DESY, Hamburg, Germany) using a wavelength of 0.9322 Å. Data processing of the (*R*)-TDPA complex was done using the XIA package and XDS[19] and of the (*S*)-TDPA complex using DENZO and SCALEPACK.[20] For statistics on data collections, see SI Table 6.

Structure Determination and Refinement. Both structures were solved by molecular replacement using MolRep implemented in the CCP4i package.[21] The structure of iGluR2-S1S2J in complex with (*S*)-2-amino-3-(3-hydroxy-4-isoxazolyl)propionic acid (PDB code 1MQD, MolA[11]) was used as search model. In the (*R*)-TDPA complex, four molecules were located in the asymmetric unit of the crystal, whereas three molecules were found in the (*S*)-TDPA complex. The program ARP/wARP[22] was used for tracing the majority of the residues. The electron densities corresponding to (*R*)-TDPA and (*S*)-TDPA were well defined (SI Figure 4). Refinements alternating with manual model building were performed using the refinement programs REFMAC5[23] and CNS[24] and the model building programs O[25] and COOT.[26] For refinement statistics, see SI Table 6.

Structure Analysis and Figure Preparation. The DynDom program[27] was used to calculate ligand-induced domain closures. The CCP4 program CONTACTS was used in the analysis of protein–ligand interactions. The program Pymol[28] was employed in the preparation of figures.

Acknowledgment. We thank O. Kristensen for help using XIA and the staff at MAX-Lab, Lund, Sweden, at BESSY, Berlin, Germany, and at EMBL, Hamburg, Germany, for help during data collection. The work was supported by grants from The Dansync Center for Synchrotron Radiation, The Danish Medical Research Council, The Lundbeck Foundation, and The European Community—Access to Research Infrastructure Action of the Improving Human Potential Programme.

Supporting Information Available: Additional information on potential hydrogen bonds, torsional angles, comparison of residues within different iGluR ligand-binding sites, details of X-ray data collection and refinements, and calculations of conformational energy penalties. This material is available free of charge via the Internet at http://pubs.acs.org.

References

(1) Bräuner-Osborne, H.; Egebjerg, J.; Nielsen, E. Ø.; Madsen, U.; Krogsgaard-Larsen, P. Ligands for glutamate receptors: design and therapeutic prospects. *J. Med. Chem.* **2000**, *43*, 2609–2645.
(2) Dingledine, R.; Borges, K.; Bowie, D.; Traynelis, S. F. The glutamate receptor ion channels. *Pharmacol. Rev.* **1999**, *51*, 7–61.
(3) Tichelaar, W.; Safferling, M.; Keinanen, K.; Stark, H.; Madden, D. R. The three-dimensional structure of an ionotropic glutamate receptor reveals a dimer-of-dimers assembly. *J. Mol. Biol.* **2004**, *344*, 435–442.
(4) Armstrong, N.; Gouaux, E. Mechanisms for activation and antagonism of an AMPA-sensitive glutamate receptor: crystal structures of the GluR2 ligand binding core. *Neuron* **2000**, *28*, 165–181.
(5) Hogner, A.; Kastrup, J. S.; Jin, R.; Liljefors, T.; Mayer, M. L.; Egebjerg, J.; Larsen, I. K.; Gouaux, E. Structural basis for AMPA receptor activation and ligand selectivity: crystal structures of five agonist complexes with the GluR2 ligand binding core. *J. Mol. Biol.* **2002**, *322*, 93–109.
(6) Jin, R.; Banke, T. G.; Mayer, M. L.; Traynelis, S. F.; Gouaux, E. Structural basis for partial agonist action at ionotropic glutamate receptors. *Nat. Neurosci.* **2003**, *6*, 803–810.
(7) Frandsen, A.; Pickering, D. S.; Vestergaard, B.; Kasper, C.; Nielsen, B. B.; Greenwood, J. R.; Campiani, G.; Fattorusso, C.; Gajhede, M.; Schousboe, A.; Kastrup, J. S. Tyr702 is an important determinant of agonist binding and domain closure of the ligand-binding core of GluR2. *Mol. Pharmacol.* **2005**, *67*, 703–713.
(8) Hogner, A.; Greenwood, J. R.; Liljefors, T.; Lunn, M. L.; Egebjerg, J.; Larsen, I. K.; Gouaux, E.; Kastrup, J. S. Competitive antagonism of AMPA receptors by ligands of different classes: crystal structure of ATPO bound to the GluR2 ligand-binding core, in comparison with DNQX. *J. Med. Chem.* **2003**, *46*, 214–221.
(9) Kasper, C.; Pickering, D. S.; Mirza, O.; Olsen, L.; Kristensen, A. S.; Greenwood, J. R.; Liljefors, T.; Schousboe, A.; Watjen, F.; Gajhede, M.; Sigurskjold, B. W.; Kastrup, J. S. The structure of a mixed GluR2 ligand-binding core dimer in complex with (*S*)-glutamate and the antagonist (*S*)-NS1209. *J. Mol. Biol.* **2006**, *357*, 1184–1201.
(10) Johansen, T. N.; Janin, Y. L.; Nielsen, B.; Frydenvang, K.; Brauner-Osborne, H.; Stensbøl, T. B.; Vogensen, S. B.; Madsen, U.; Krogsgaard-Larsen, P. 2-Amino-3-(3-hydroxy-1,2,5-thiadiazol-4-yl)propionic acid: resolution, absolute stereochemistry and enantiopharmacology at glutamate receptors. *Bioorg. Med. Chem.* **2002**, *10*, 2259–2266.
(11) Kasper, C.; Lunn, M.-L.; Liljefors, T.; Gouaux, E.; Egebjerg, J.; Kastrup, J. S. GluR2 ligand-binding core complexes: importance of the isoxazolol moiety and 5-substituent for the binding mode of AMPA-type agonists. *FEBS Lett.* **2002**, *531*, 173–178.
(12) Lunn, M. L.; Hogner, A.; Stensbøl, T. B.; Gouaux, E.; Egebjerg, J.; Kastrup, J. S. Three-dimensional structure of the ligand-binding core of GluR2 in complex with the agonist (*S*)-ATPA: implications for receptor subunit selectivity. *J. Med. Chem.* **2003**, *46*, 872–875.
(13) Naur, P.; Vestergaard, B.; Skov, L. K.; Egebjerg, J.; Gajhede, M.; Kastrup, J. S. Crystal structure of the kainate receptor GluR5 ligand-binding core in complex with (*S*)-glutamate. *FEBS Lett.* **2005**, *579*, 1154–1160.
(14) Mayer, M. L. Crystal structures of the GluR5 and GluR6 ligand binding cores: molecular mechanisms underlying kainate receptor selectivity. *Neuron* **2005**, *45*, 539–552.
(15) Johansen, T. N.; Greenwood, J. R.; Frydenvang, K.; Madsen, U.; Krogsgaard-Larsen, P. Stereostructure−activity studies on agonists at the AMPA and kainate subtypes of ionotropic glutamate receptors. *Chirality* **2003**, *15*, 167–179.

(16) Chen, G. Q.; Sun, Y.; Jin, R.; Gouaux, E. Probing the ligand binding domain of the GluR2 receptor by proteolysis and deletion mutagenesis defines domain boundaries and yields a crystallizable construct. *Protein Sci.* **1998**, *7*, 2623–2630.
(17) Madsen, U.; Pickering, D. S.; Nielsen, B.; Bräuner-Osborne, H. 4-Alkylated homoibotenic acid (HIBO) analogues: versatile pharmacological agents with diverse selectivity profiles towards metabotropic and ionotropic glutamate receptor subtypes. *Neuropharmacology* **2005**, *49*, 114–119.
(18) Nielsen, B. B.; Pickering, D. S.; Greenwood, J. R.; Brehm, L.; Gajhede, M.; Schousboe, A.; Kastrup, J. S. Exploring the GluR2 ligand-binding core in complex with the bicyclical AMPA analogue (*S*)-4-AHCP. *FEBS J.* **2005**, *272*, 1639–1648.
(19) Bahar, M.; Ballard, C.; Cohen, S. X.; Cowtan, K. D.; Dodson, E. J.; Emsley, P.; Esnouf, R. M.; Keegan, R.; Lamzin, V.; Langer, G.; Levdikov, V.; Long, F.; Meier, C.; Muller, A.; Murshudov, G. N.; Perrakis, A.; Siebold, C.; Stein, N.; Turkenburg, M. G.; Vagin, A. A.; Winn, M.; Winter, G.; Wilson, K. S. SPINE workshop on automated X-ray analysis: a progress report. *Acta Crystallogr., Sect. D: Biol. Crystallogr.* **2006**, *62*, 1170–1183.
(20) Otwinowski, Z.; Minor, W. Processing of X-ray diffraction data collected in oscillation mode. *Methods Enzymol.* **1997**, *276*, 307–326.
(21) Collaborative Computational Project, Number 4. The CCP4 Suite: Programs for Protein Crystallography. *Acta Crystallogr., Sect. D: Biol. Crystallogr.* **1994**, *50*, 760–763.
(22) Perrakis, A.; Morris, R.; Lamzin, V. S. Automated protein model building combined with iterative structure refinement. *Nat. Struct. Biol.* **1999**, *6*, 458–463.
(23) Murshudov, G. N.; Vagin, A. A.; Dodson, E. J. Refinement of macromolecular structures by the maximum-likelihood method. *Acta Crystallogr., Sect. D: Biol. Crystallogr.* **1997**, *53*, 240–255.
(24) Brünger, A. T.; Adams, P. D.; Clore, G. M.; DeLano, W. L.; Gros, P.; Grosse-Kunstleve, R. W.; Jiang, J.-S.; Kuszewski, J.; Nilges, M.; Pannu, N. S. Crystallography and NMR system: a new software suite for macromolecular structure determination. *Acta Crystallogr., Sect. D: Biol. Crystallogr.* **1998**, *54*, 905–921.
(25) Jones, T. A.; Zou, J. Y.; Cowan, S. W.; Kjeldgaard, M. Improved methods for building protein models in electron density maps and the location of errors in these models. *Acta Crystallogr.* **1991**, *A47*, 110–119.
(26) Emsley, P.; Cowtan, K. Coot: Model-building tools for molecular graphics. *Acta Crystallogr., Sect. D: Biol. Crystallogr.* **2004**, *60*, 2126–2132.
(27) Hayward, S.; Lee, R. A. Improvements in the analysis of domain motions in proteins from conformational change: DynDom version 1.50. *J. Mol. Graphics Modell.* **2002**, *21*, 181–183.
(28) DeLano, W. L. *The PyMOL Molecular Graphics System*; DeLano Scientific: Palo Alto, CA, 2002.

JM701126W